CHAPTER 9

Inhibition of $A\beta_{1-42}$ peptide aggregation using short ss-oligonucleotide as polyions: An *in silico* approach

Inhibition of $A\beta_{1-42}$ peptide aggregation using short ss-oligonucleotide as polyions: An *in silico* approach

9.1. Abstract:

Prevention or reduction of the aggregation process in $A\beta_{1-42}$ peptide is foreseen as a potential therapeutic approach. Many methods have been studied to reduce the aggregation of $A\beta_{1-42}$ peptide. Recently the role of polyions has been highlighted in the inhibition of fibril formation and fibril disassembly. In this perspective, the present study focuses on investigating the interaction between the $A\beta_{1-42}$ peptide and short single stranded (ss)-oligonucleotide. The findings reported herein state that the $A\beta_{1-42}$ peptide monomer in presence of the ss-oligonucleotide retains its α-helical conformation and the ss-oligonucleotide encapsulate the $A\beta_{1-42}$ peptide and prevent the dimer formation by inhibiting the approach of another monomeric unit through electrostatic interactions. We also observed ss-oligonucleotide to play a significant role in the disassembly of $A\beta_{17-42}$ dimer by destabilizing the interaction between the β-strands. Our findings in this study may be considered useful in the development of a method for the inhibition of the $A\beta_{1-42}$ peptide aggregation at an early stage, thereby reducing the risk of AD that concerns an ever aging population.

9.2. Introduction:

Different methods to inhibit or modify the formation of the soluble intermediate species will be the first step to AD's treatment. While the pathophysiology of AD is not fully understood, numerous studies have been carried out to shed light on the aggregation mechanisms of $A\beta_{1-42}$ peptide and its inhibition. $A\beta_{1-42}$ peptide aggregation can be inhibited at different stages. During nucleation, inhibitors can bind to monomers and prevent their secondary structural transitions, or from forming dimers. Inhibitors can also bind to free ends of growing nuclei and block further elongation. Effective therapeutic strategies must be designed targeting accurate minute steps during the $A\beta_{1-42}$ peptide aggregation process. Many strategies have been developed to inhibit the aggregation process of $A\beta_{1-42}$ peptide which is discussed in introductory chapter. In our work we have approached in four different ways to inhibit the early and late stage aggregation of $A\beta_{1-42}$ peptide which is discussed below. In our first approach we used ss-oligonucleotide as an inhibitor.

Recent studies have reported interaction of amyloid fibrils with polyanions such as DNA, ATP and heparin [225-228]. Conjugation of nucleotide sequence with peptide sequence to form DNA–peptide hybrid which self-assemble in aqueous solution has been investigated recently [229, 230]. Moreover, Abraham and his coworkers has stated that on incubation of Aβ fibers with polyions, inhibition of amyloid fibril genesis as well as disassembly of fibers take place [231]. Their results were supported by experimental techniques including AFM and TEM imaging and CD and FTIR spectroscopy. In the present study, we have focused on inhibiting the $A\beta_{1-42}$ peptide aggregation at its initial stage using ss-oligonucleotide. Furthermore, we have also examined the inhibitory effect of ss-oligonucleotide on the $A\beta_{17-42}$ dimer.

9.3. Materials & Methods:

9.3.1. Building ss-oligonucleotide from Nucleic acid builder (NAB):

Using the NAB, small modelling language, we built two ss-oligonucleotides. One of 12-mer 5' AAA GAG AGA GAG 3' and the other of 18-mer 5' AAA GAG AGA GAG AAA GAG 3'. ASCII-art was used to depict duplexes. The make-na text parser and modelling code is open source and available under the GPLv3 [232].

9.3.2. MD simulation of $A\beta_{1-42}$ peptide monomer in presence of ss-oligonucleotide:

The initial structure of $A\beta_{1-42}$ was taken from Protein Data Bank, PDB entry: 1IYT [211]. The $A\beta_{1-42}$ peptide-ss-oligonucleotide complex was built using the LEaP module of AMBER12 [169]. The $A\beta_{1-42}$ peptide-ss-oligonucleotide complex was then solvated with TIP3P water model with solvent buffer being 10 Å in all directions [170]. To neutralize the negative charge of the $A\beta_{1-42}$ peptide-ss-oligonucleotide complex Na^+ ions close to the solute surface were added. Minimization, heating and equilibration was carried out as described in Chapter 5 (section 5.3.1). Production run was carried out to collect the trajectories to generate the data. After every MD run, the VMD package was used for visualizing the trajectories generated [192].

9.3.3. MD simulation of $A\beta_{17-42}$ peptide dimer in presence of ss-oligonucleotide:

The initial dimer structure of the $A\beta_{17-42}$ peptide was constructed from the NMR fibril structure taken from the Protein Data Bank, PDB entry: 2BEG [125]. Then we

carried out the MD simulation by constructing the $A\beta_{17-42}$ dimer-ss oligonucleotide (18-mer) complex using the LEAP module and further steps were carried out as mentioned in section 9.3.2.

9.4. Results & Discussions:

9.4.1. Effect of ss-oligonucleotide on the conformations of $A\beta_{1-42}$ peptide:

We used ss-oligonucleotide as an inhibitor to $A\beta_{1-42}$ peptide aggregation and carried out interaction studies as a first step to monitor its aggregation inhibition. Moreover, we used ss-oligonucleotide to disassemble the pre-formed amyloid fibril structure. By using MD approach, we made the $A\beta_{1-42}$ peptide-ss-oligonucleotide complex and $A\beta_{17-42}$ dimer -ss-oligonucleotide complex and tried to describe the conformational features in presence of ss-oligonucleotide.

To carry out the study with $A\beta_{1-42}$ monomer, we generated the starting complex with the equilibrated structure of $A\beta_{1-42}$ peptide and ss-oligonucleotide within a distance of 10 Å. We have discussed about the initial $A\beta_{1-42}$ monomer secondary structure in Chapter 1 which is characterized by helical trait encompassing residues 8 to 25 and 28 to 38 connected by a β-turn (residue: 25-26). During the time course of simulation, it was observed that $A\beta_{1-42}$ monomer changes its secondary structural conformations from α-helix to random coils and β-strands. On the other hand, in presence of ss-oligonucleotide, $A\beta_{1-42}$ monomer retained its initial secondary structure and was stable throughout the simulation run. In **Figure 9.1** we can see snapshots of the $A\beta_{1-42}$ monomer in presence of ss-oligonucleotide at different intervals which show most of the residues to be in α-helical conformation.

9.4.2. Secondary structural analysis of $A\beta_{1-42}$ peptide in presence of ss-oligonucleotide:

The probability score graph results are also in good agreement with the assessment that ss-oligonucleotide supports in retaining the native structure of $A\beta_{1-42}$ monomer (**Figure 9.2**). From the graph we can observe that, most of the residues retained their α-helical conformation in presence of the ss-oligonucleotide. Also, the ss-oligonucleotide encapsulates the $A\beta_{1-42}$ peptide and prevents another monomeric unit from binding and hence dimer formation is inhibited. This can be attributed to the

electrostatic interaction between the ss-oligonucleotide and positively charged residues of $A\beta_{1-42}$ peptide.

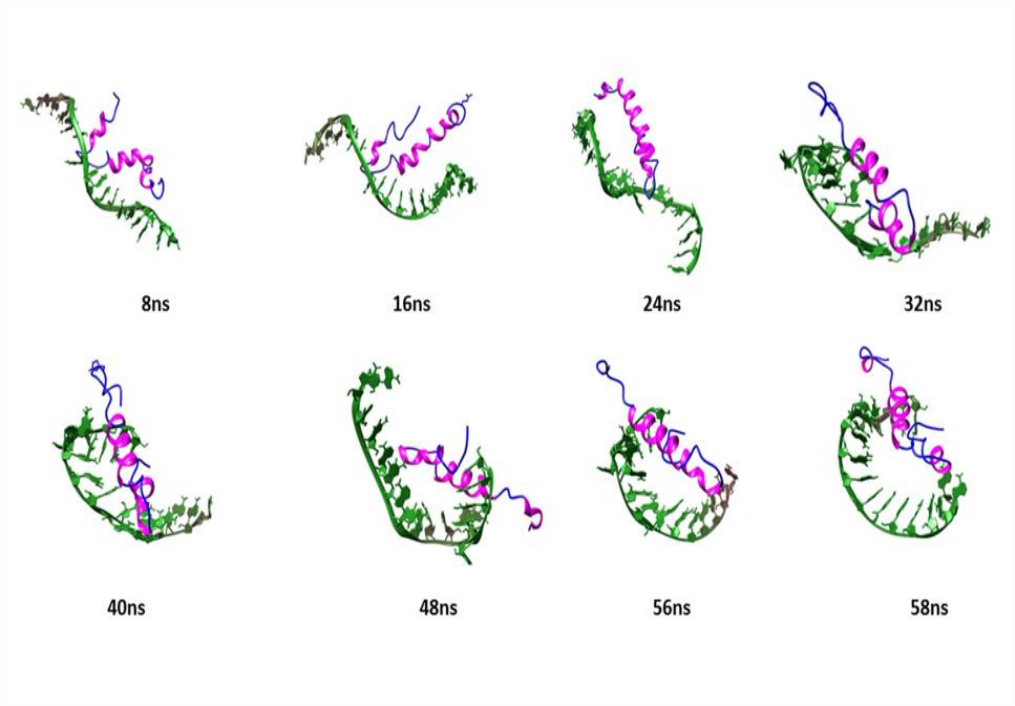

Figure 9.1. *Snapshots of $A\beta_{1-42}$ peptide in presence of ss-oligonucleotide at 300 K during the time course of simulation period.*

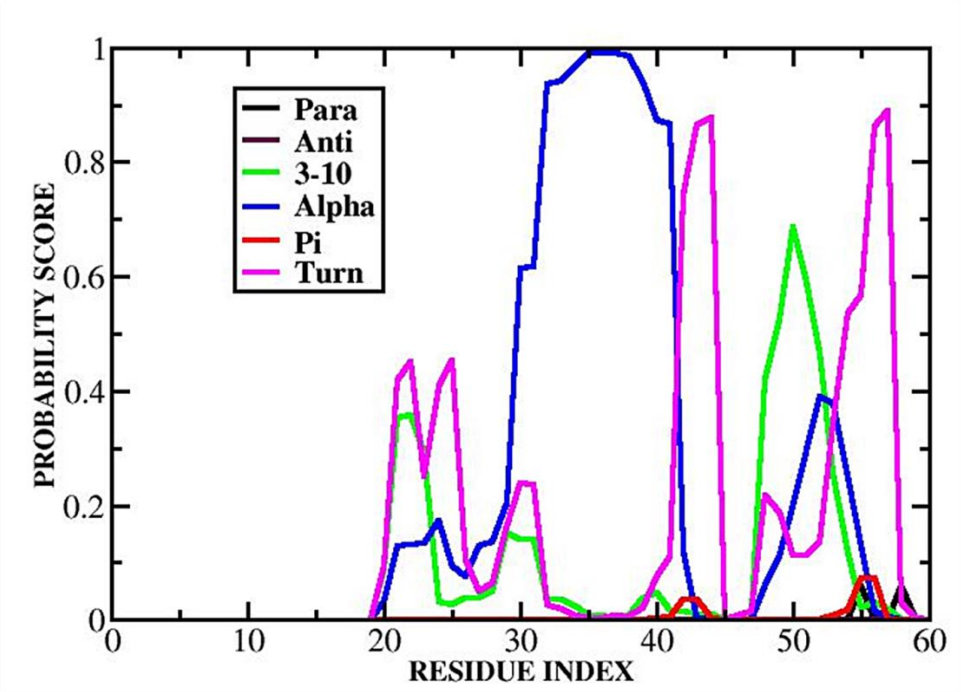

Figure 9.2. *Probability score of secondary structure for each residue in the $A\beta_{1-42}$ peptide in presence of ss-oligonucleotide.*

We also carried out the simulation using 12-mer ss-oligonucleotide wherein we observed similar results **(Figure 9.3).** This shows that the interaction between ss-oligonucleotide and $A\beta_{1-42}$ peptide is sequence independent.

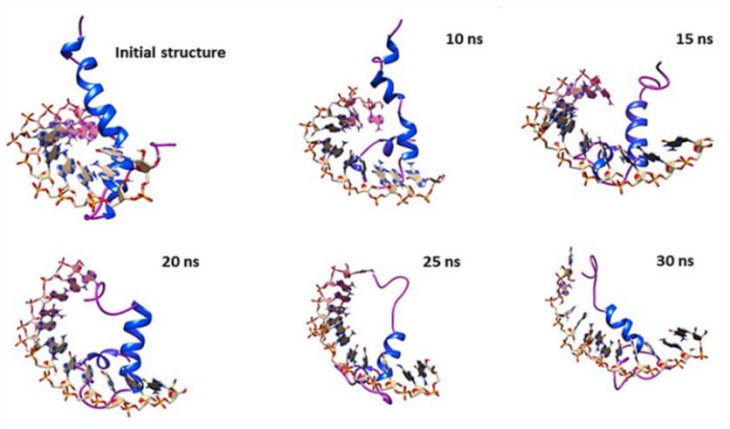

***Figure 9.3**. Snapshots of $A\beta_{1-42}$ peptide at 300 K during the time course of simulation period in presence of 12-mer ss-oligonucleotide.*

We then examined the evolution of secondary structural elements during the simulations. **Figure 9.4** shows the classification of the trajectories in terms of secondary-structure elements obtained by the software tool DSSP [183] which assigns secondary structures to the amino acids of a protein, by identifying the intra-backbone hydrogen bonds of the protein. From the plot we can see the stability (or de-stability) of secondary structure elements as a function of time. Examination of **Figure 9.4** shows that the main features of the α-helix structure were largely retained.

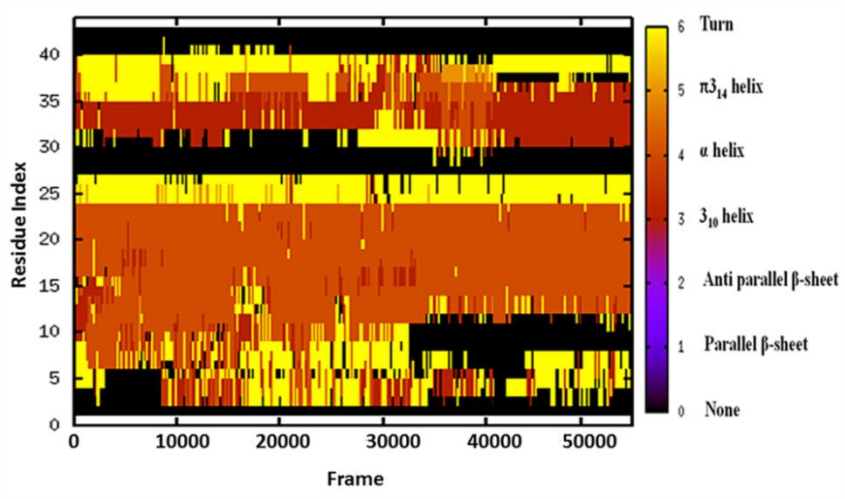

***Figure 9.4.** Time evolution of secondary structure of $A\beta_{1-42}$ peptide in presence of ss-oligonucleotide at 300 K.*

9.4.3. Stability of $A\beta_{1-42}$ peptide in presence of ss-oligonucleotide:

To check the conformational stabilities of the $A\beta_{1-42}$ peptide in presence of ss-oligonucleotide the RMSDs of the C-α atoms with respect to the minimized starting structure, radius of gyration (Rg) and B Factor Value of the corresponding backbones with respect to their energy minimized structure were calculated and monitored over the course of simulations and are presented in **Figure 9.5**. Assessment of the structural drift was carried out by analyzing the C-α atom RMSDs. We found that the backbone RMSDs of the peptide deviated up to 5 ns and then the structure converged and attained almost stable conformation (**Figure 9.5. A)**.

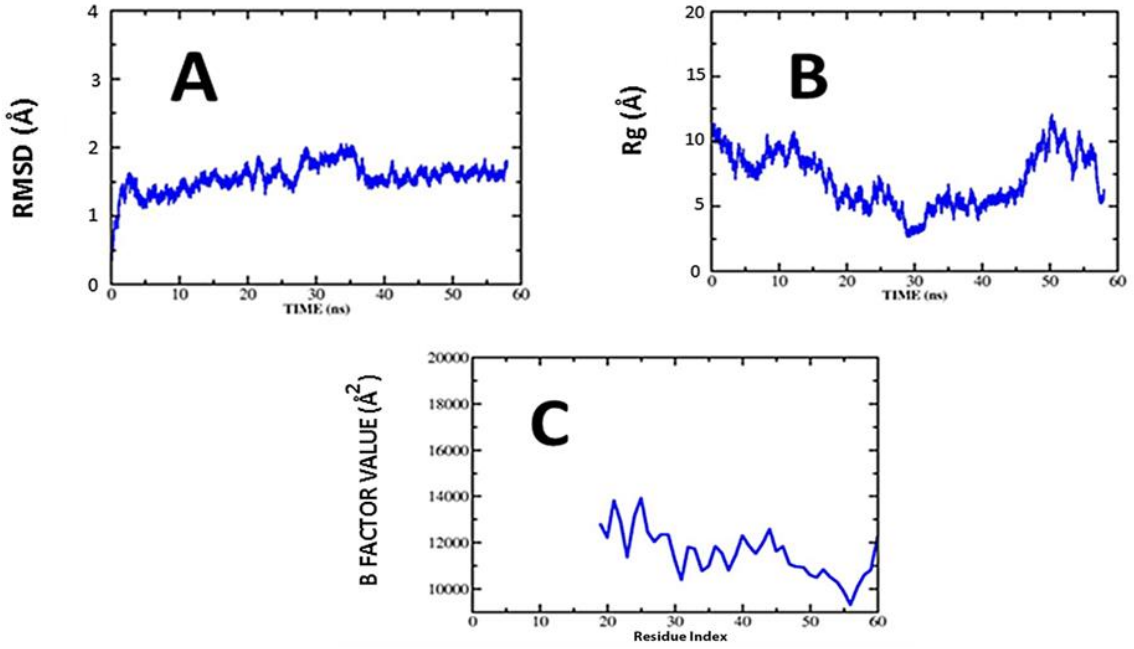

Figure 9.5*. A) Backbone RMSD vs time Course of simulation period; B) Radius of Gyration as a function of time course of simulation; C) B-Factor value of C-α atoms for each residue using the backbone atomic fluctuation as a function of amino acids for the $A\beta_{1-42}$ peptide in presence of ss-oligonucleotide.*

From the RMSD plot, we can infer that $A\beta_{1-42}$ peptide structure underwent structural changes through the initial 5 ns time period and then reached the equilibration. The stability of the peptide was due to its ability to retain its native α-helical conformation in presence of ss-oligonucleotide. The B Factor Value and Rg are related to the general tertiary structure of the protein. **Figure 9.5.B** shows the radius of gyration of peptide backbone as a function of time. In the simulation carried out, the

radius of gyration oscillated to a greater degree before 5 ns, further confirming that the peptide structure remained stable after 5 ns from the simulation being initiated. **Figure 9.5.C** shows the local dynamics and flexibility of each part of the $A\beta_{1-42}$ peptide. From the plot we can notice that the N-terminal region exhibited a high flexibility by changing its conformation from helix to random coils. This is in agreement with the RMSD result above.

9.4.4. Hydrophobic contacts and hydrogen bonding analysis of $A\beta_{1-42}$ peptide and the ss-oligonucleotide:

Proteins interact with DNA through different energetic factors which include similar physical forces which include electrostatic interactions (salt bridges), dipolar interactions (hydrogen bonding), entropic effects (hydrophobic interactions) and dispersion forces (base stacking). We thus calculated the total number of hydrophobic contacts and the hydrogen bonds involved in the interaction between $A\beta_{1-42}$ peptide and the ss-oligonucleotide. **Figure 9.6** shows the total number of hydrogen bonds and hydrophobic contacts as a function of time between the $A\beta_{1-42}$ peptide and the ss-oligonucleotide. Hydrogen bonds formed thus stabilize the $A\beta_{1-42}$ peptide-ss-oligonucleotide complex in the final state via favorable interactions.

9.4.5. Effect of ss-oligonucelotide on conformations of $A\beta_{17-42}$ peptide dimer:

Furthermore, studies on the disassembly of the dimeric unit by the ss-oligonucelotide (18-mer) were also carried out. The initial ss-oligonucleotide -$A\beta_{17-42}$ dimer complex is shown in **Figure 9.7.A**, which displays β-strands at specific regions. ss-oligonucleotide acts as a β-sheet breaker and disassembles the β-stranded dimeric unit. From **Figure 9.7.B**, we can observe that the β-strands undergo a radical change upon the interaction with the ss-oligonucleotide and finally result in helical twists in the now disoriented $A\beta_{17-42}$ dimer.

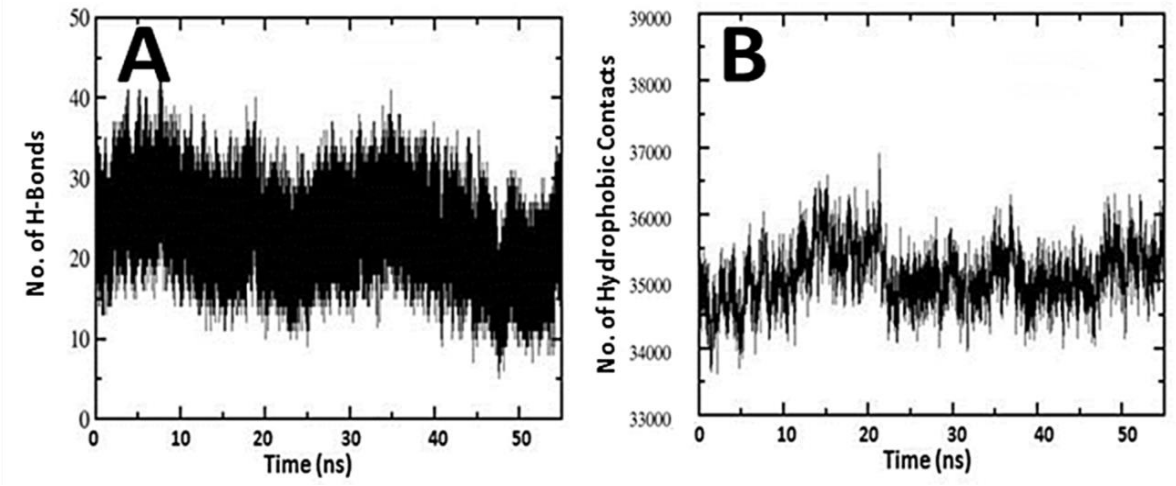

Figure 9.6.*A) Total number of hydrogen bonds; B) total number of hydrophobic contacts vs time Course of simulation period for the* $A\beta_{1\text{-}42}$ *peptide in presence of ss-oligonucleotide.*

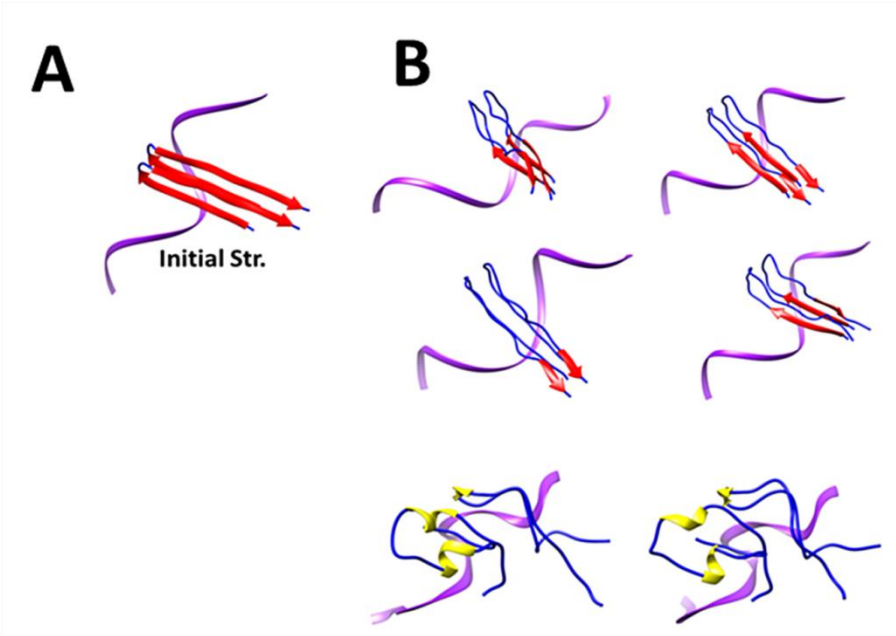

Figure 9.7.*A) Initial structure of* $A\beta_{17\text{-}42}$ *dimer-ss-oligonucleotide complex; B) snapshots of* $A\beta_{17\text{-}42}$ *dimer at 300 K during the time course of simulation period in presence of ss-oligonucleotide.*

9.4.6. Hydrophobic contacts and hydrogen bonding analysis of $A\beta_{17-42}$ peptide dimer and the ss-oligonucleotide:

Similar to that of $A\beta_{1-42}$ peptide, in case of $A\beta_{17-42}$ dimer also we have calculated the total number of hydrophobic contacts and hydrogen-bonds formed between the ss-oligonucelotide and the $A\beta_{17-42}$ dimer (**Figure 9.8**). A large number of hydrophobic contacts were found to be present between the $A\beta_{17-42}$ dimer and the ss-oligonucleotide, which is indicative of the hydrophobic interactions between the ss-oligonucleotide and the $A\beta_{17-42}$ dimer (**Figure 9.8.A**). We also observed a higher percentage of hydrogen bonds that were formed between the $A\beta_{17-42}$ dimer and the ss-oligonucleotide (**Figure 9.8. B**). The higher percentages of hydrogen bonds were found to stabilize the final $A\beta_{17-42}$ dimer - ss-oligonucleotide complex.

9.4.7. Binding energetics of ss-oligonucleotide with $A\beta_{1-42}$ peptide:

To evaluate quantitatively the change of the $A\beta_{1-42}$ peptide structure, we calculate the energetics in terms of *van der Waals* and electrostatic interaction (**Figure 9.9**). Specificity of the interaction between the ss-oligonucleotide and the peptide was manifested on both the electrostatic energy and the *van der Waals* force. In case of $A\beta_{1-42}$ peptide-ss-oligonucleotide complex, the electrostatic energy displayed higher negative value while *van der Waals* shows positive values (**Figure 9.9.A & B**). The negative electrostatic energy and a positive *van der Waals* force lead the complex to have a favorable electrostatic interaction. **Figure 9.9.C & D** shows the electrostatic energy and the *van der Waals* force of $A\beta_{17-42}$ dimer-ss-oligonucleotide complex. From the figure we can observe negative values for both the energetics, thus indicating that the $A\beta_{17-42}$ dimer-ss-oligonucleotide complex exhibits both electrostatic interaction as well as *van der Waals* force.

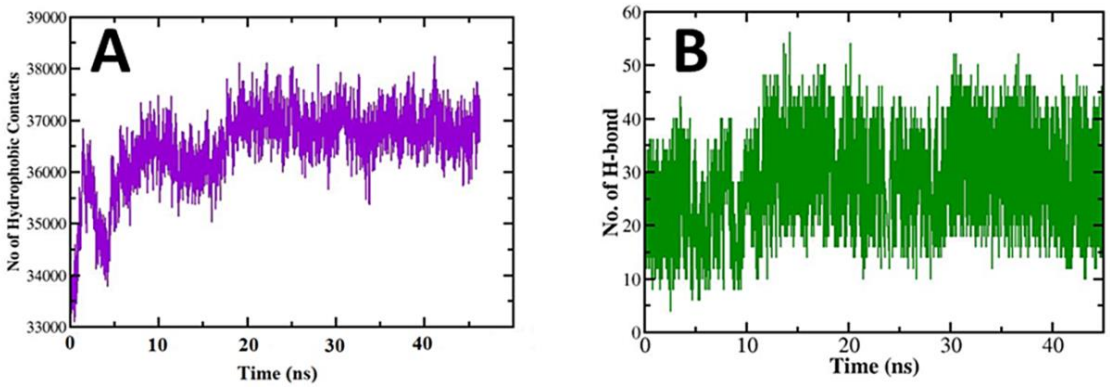

Figure 9.8. *A) Total number of hydrophobic contacts; B) Total number of hydrogen bonds vs time course of simulation period for the Aβ17-42 dimer in presence of ss-oligonucleotide.*

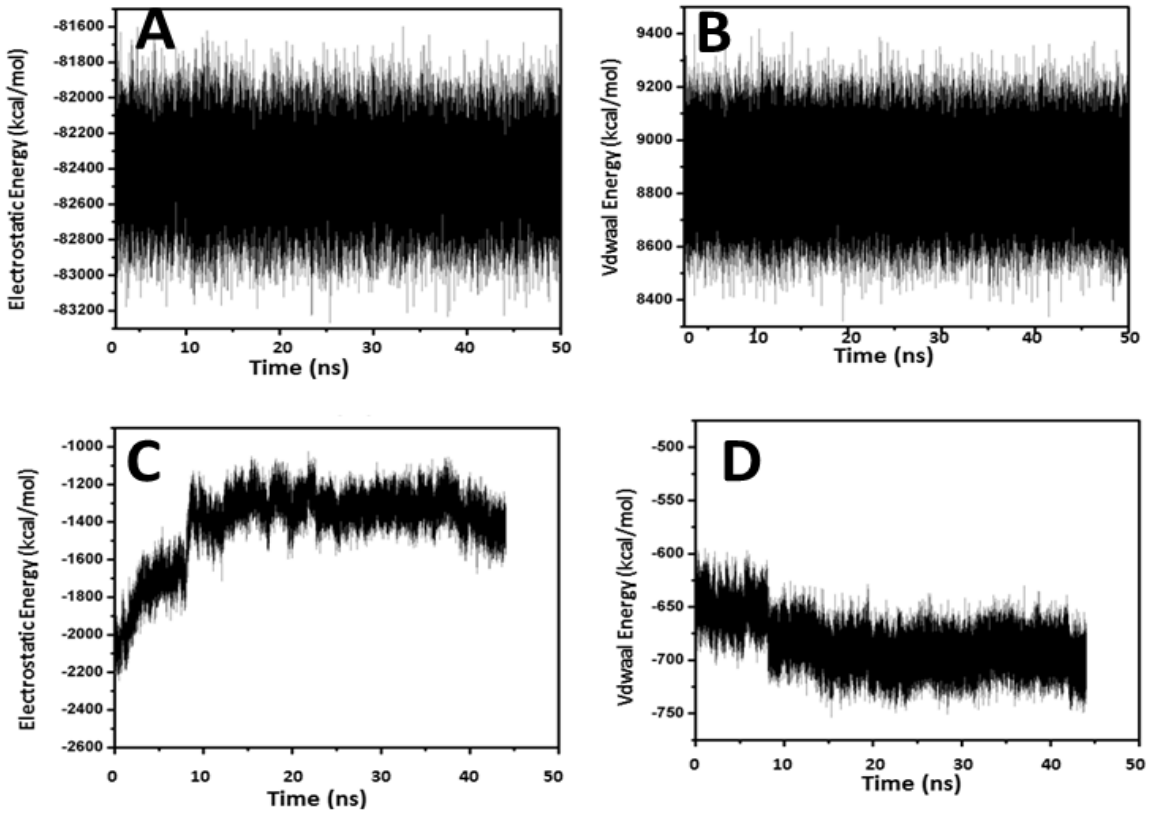

Figure 9.9. *A) Electrostatic Energy; B) Vdwaal Energy vs time course of simulation period for the Aβ1-42 peptide in presence of ss-oligonucleotide; C) Electrostatic Energy; D) VdWaal Energy vs time course of simulation period for the Aβ17-42 dimer in presence of ss-oligonucleotide.*

9.5. Conclusions:

The current work hereby describes the characteristic features of the $A\beta_{1-42}$ peptide, a major risk factor for the onset of AD, in the presence of ss- oligonucleotide. In the current study we report that the $A\beta_{1-42}$ peptide retains its α-helical structure in presence of ss-oligonucleotide thus preventing the formation of dimers further downstream. Herein, the ss- oligonucleotide was found to encapsulate the $A\beta_{1-42}$ peptide monomer via electrostatic interactions, thus resulting in the aversion of the dimerization process by preventing the approach of other monomeric units from binding to the existing $A\beta_{1-42}$ peptide. We have also demonstrated that the ss-oligonucleotide facilitates the disassembly of $A\beta_{17-42}$ dimer, which was attributed to electrostatic interactions, hydrogen bonds and to the hydrophobic interactions between the $A\beta_{17-42}$ dimer and the ss-oligonucleotide. These forces were found to contribute in varying degrees to the disassembly of the amyloid beta dimer in a sequence and length independent manner. We hope that the findings of our work are of significant interest for the development of novel approaches that will inhibit the $A\beta_{1-42}$ peptide aggregation at an early stage thereby reducing the risk of AD that concerns an ever aging population.